TYPE Original Research
PUBLISHED 14 October 2025
DOI 10.3389/feart.2025.1694288



OPEN ACCESS

EDITED BY
Qingchao Li,
Henan Polytechnic University, China

REVIEWED BY
Zhengzheng Cao,
Henan Polytechnic University, China
Xianyu Yang,
China University of Geosciences, China

*CORRESPONDENCE
Penghao Lin,

☑ linpenghao333@163.com

RECEIVED 30 August 2025 ACCEPTED 29 September 2025 PUBLISHED 14 October 2025

CITATION

Lin P (2025) Damage mechanism and protection measures for Yanchang shale Chang 7 reservoir, China. *Front. Earth Sci.* 13:1694288. doi: 10.3389/feart.2025.1694288

COPYRIGHT

© 2025 Lin. This is an open-access article distributed under the terms of the Creative Commons Attribution License (CC BY). The use, distribution or reproduction in other forums is permitted, provided the original author(s) and the copyright owner(s) are credited and that the original publication in this journal is cited, in accordance with accepted academic practice. No use, distribution or reproduction is permitted which does not comply with these terms.

Damage mechanism and protection measures for Yanchang shale Chang 7 reservoir, China

Penghao Lin*

CCTEG Coal Mining Research Institute, Beijing, China

The Yanchang shale is a key resource in the Ordos Basin of Shaanxi, China. To optimize its extraction and production, it is crucial to understand formation damage mechanisms and implement effective solutions. In this study, shale samples were analyzed for mineral composition and microstructure using X-ray diffraction and scanning electron microscopy. Hydration characteristics were evaluated through inhibition tests, and the water contact angle on the shale was measured. Changes in shale permeability were determined via pressure transmission tests. The results identified that water blocking, polymer intrusion, water sensitivity and salt sensitivity as the primary causes of reservoir damage. To address these issues, a surfactant was proposed to modify core wettability and eliminate water blockage, while an enzyme was suggested to prevent polymer wrapping and clogging. Incorporating these additives can lead to the development of low-damage fracturing fluid systems that enhance performance.

KEYWORDS

Yanchang shale, damage mechanism, reservoir sensitivity, water blocking, polymer degradation

1 Introduction

Shale gas, which is a natural gas trapped within dense organic-rich shale formations, has emerged as a crucial component of the global energy supply, significantly contributing to the diversification of natural gas supplies (International Energy Agency IEA, 2011; Dai et al., 2019). Unlike conventional reservoirs, shale formations are characterized by nanoscale pore systems and extremely low permeability, making gas extraction particularly challenging (Cadwallader et al., 2015; Duan et al., 2022; Chaturvedi et al., 2019; Wang et al., 2025). Economic production relies heavily on horizontal drilling combined with hydraulic fracturing to enhance recovery efficiency (Li et al., 2025a; Tao et al., 2022; Azim et al., 2024). However, field observations indicated that water-based fracturing fluids and associated additives can induce significant formation damage, impairing both permeability and fracture conductivity, and consequently reducing gas production efficiency.

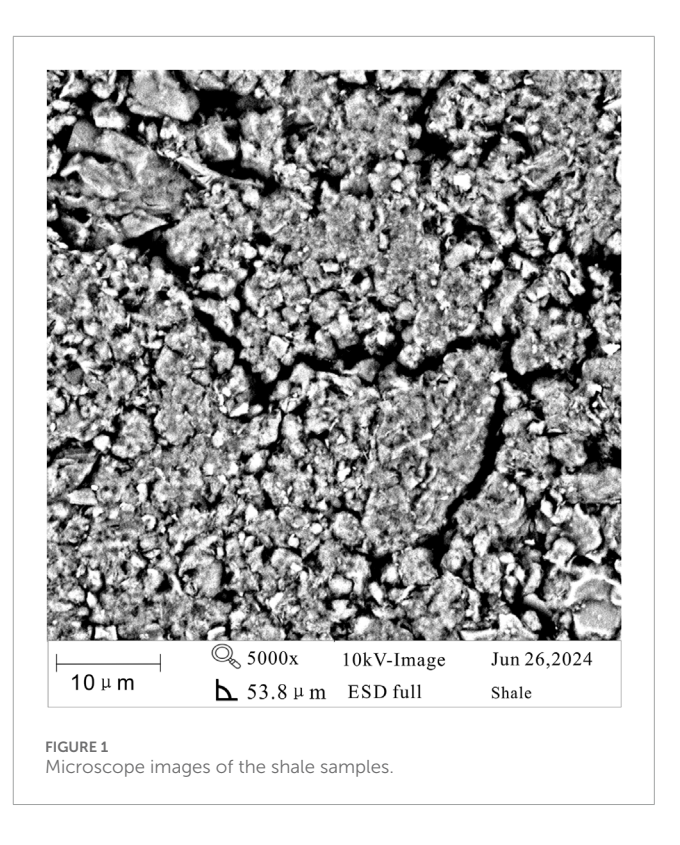
Formation damage, an undesirable reduction in rock permeability can occur throughout various operational phases, including drilling, pumping, and hydraulic fracturing (Liu et al., 2020; Li et al., 2023; Li, 2025). This damage diminishes the natural productivity of reservoir rocks (Shi et al., 2022) and arises through two primary mechanisms: physical and chemical (Wang et al., 2013). Physical damage results from direct interactions between

the formation and working fluids (e.g., drill-in, completion, or fracturing fluids), leading to phenomena such as fines migration, particle intrusion, and stress-induced damage (Shao et al., 2021; Nwabia and Leung, 2024). Chemical damage stems from incompatibilities between formation minerals and working fluids, manifesting as clay swelling, dispersion due to water sensitivity, and permeability reduction caused by salinity sensitivity. Of these water sensitivity caused by clay-fluids interactions represents one of the most common damage mechanisms in shale reservoirs (Xu et al., 2023; Yang et al., 2020).

Extensive research on damage mechanisms has been conducted in marine shale formations, largely informed by North American shale development experiences. Studies emphasize the critical role of fluid-shale interactions in altering pore networks and impeding gas transport (Yang et al., 2018; Li et al., 2020). For example, Bal and Misra (Bal and Misra, 2024) performed laboratory evaluations of shale sensitivity and proposed a high-pH oil-based drilling fluid to enhance emulsion stability. Their results showed permeability reductions of up to 57.0% and 88.5% due to water and alkali sensitivity, respectively. Such impairments reduce the hydraulic width of fractures, thereby decreasing fracture conductivity and overall reservoir permeability (Yi et al., 2021; Ngata et al., 2022; Li et al., 2025b). Guo et al. (2022) identified water blocking and gel residue as major contributors to permeability damage in the Wangfu shale deposit. By applying a low-concentration guar gum fluid enhanced with anionic surfactants, they achieved a 91% recovery of core gas permeability. Chen et al. (2021) developed a fuzzy analytic hierarchy model incorporating petrophysical properties and multiscale flow properties to evaluate formation damage in Longmaxi shale, revealing damage levels of 65% in the matrix and 84% within fractures.

Despite these advances in understanding marine shales, research on continental shale formations remains limited, particularly in the context of China's continental shale resources, which have not yet achieved widespread commercial development. The Yanchang shale gas reservoir, situated in the northeastern Ordos Basin, represents one of the most promising targets for continental shale gas exploration in China. Over recent decades, this basin has witnessed a growing number of gas-producing wells and several major breakthrough discoveries (Wang et al., 2020). Unlike the more established shale gas industries such as the Longmaxi shale in Southwest China, gas production from continental shale reservoirs has been limited. This underperformance highlights the need for a thorough investigation of the Chang 7 member of the Yanchang shale.

This study aims to examine the formation damage mechanisms in continental shale gas reservoirs by analyzing shale pore structure and sensitivity characteristics. Focusing on the Chang 7 member of the Yanchang Formation, the impact of various fracturing fluids on shale permeability and propose optimized low-damage fluid formulation to enhance production performance. This study is intended to provide theoretical and practical insights for the efficient development of continental shale gas resources.



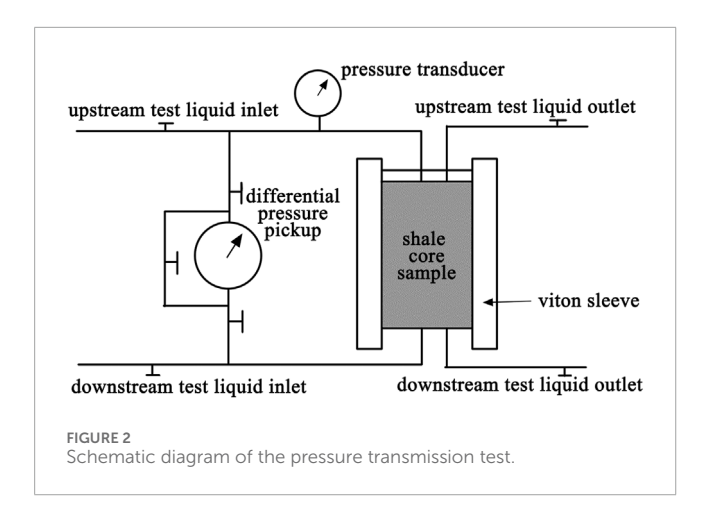
2 Materials and experimental methods

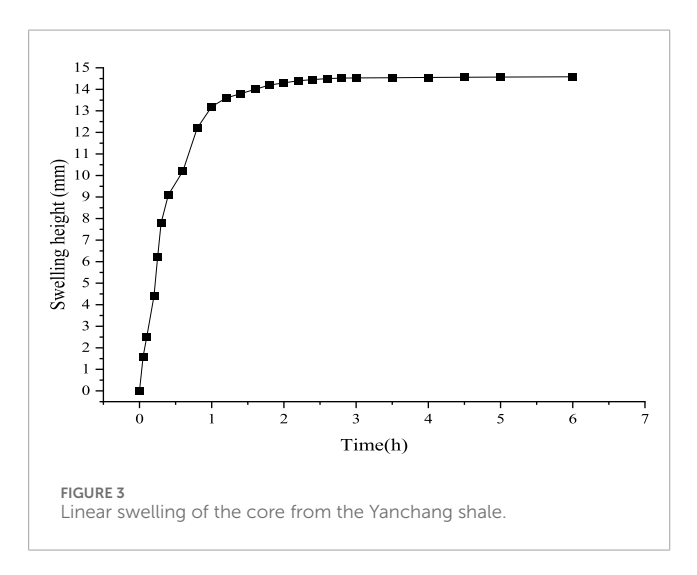
2.1 Shale used

Shale core samples were collected from an outcrop of the Chang 7 member of the Yanchang Formation, Ordos Basin, located in Northwest China. All cores were machined to a uniform diameter and height to ensure experimental reproducibility. Mineralogical analysis via X-ray diffraction (XRD) revealed that the shale is predominantly composed of quartz (up to 43%), along with significant clay minerals, including illite (28%) and chlorite (21%), as well as feldspar. The substantial clay content, particularly the high proportions of illite and chlorite, suggests a pronounced susceptibility to water sensitivity and moderate brittleness (Guo et al., 2018), both of which are critical factors influencing hydraulic fracturing performance.

The pore structure plays a fundamental role in fluid transport and long-term productivity in shale gas reservoirs. To determine the microfracture morphology of the reservoir, fresh sample surfaces were observed using scanning electron microscopy (SEM). Representative images are provided in Figure 1.

As shown in Figure 1, the shale samples exhibit a well-developed system of microcracks, with widths ranging from 0.2 to 2 μm . These microfractures exhibit curved and branching morphologies with considerable variability in geometry. The matrix is unevenly distributed and largely fragmented into particles and aggregates by fine cracks. Quartz crystals are dispersed throughout the matrix, while clay minerals occupy the spaces between quartz particles, infilling the pores and fissures. This microstructure suggests that the reservoir is potentially fracturable, while also underscoring the importance of accounting for capillary effects associated with





variations in microfracture geometry during reservoir development to mitigate water-blocking damage.

2.2 Experimental methods

2.2.1 Inhibition test

The water absorption characteristics of the shale samples were measured using linear expansion experiments (Zhang et al., 2024). This method compresses shale powder into standard cores, exposes them to test liquids under constant axial confinement, and continuously monitors longitudinal height changes caused by water absorption with high-precision displacement sensors. First, the shale was crushed, ground, and sieved to obtain powder smaller than 80 mesh. The powder was dried in a constant-temperature oven at 105 °C for 4 h, then cooled to room temperature. Next, 10 g of shale powder was precisely weighed into a mold and compressed at 1.5 MPa for 15 min to form a dense, standard cylindrical core with an initial height of 11.5 mm. All cores were formed in a single compression to minimize errors.

The compressed core was carefully placed into the ZNP-1 expansion tester's sample chamber, ensuring fully contact between the core's top surface and the piston probe. A fixed axial load

was applied to simulate slight subsurface confinement. Test fluid was slowly injected to fully submerge the core. Once activated, the instrument automatically recorded the core's expansion height every 2 s for 24 h.

2.2.2 Pressure transmission test

Pressure transmission testing replicates the pressure differential between the wellbore and formation by applying pressure across the shale sample. While maintaining constant upstream pressure, sensors monitor dynamic pressure changes in the sealed fluids at both ends. Figure 2 illustrates the experimental setup: the shale sample is placed between two porous screens inside a Viton sleeve that applies radial confining stress. The hollow piston connects to a downstream reservoir equipped with a pressure sensor.

With the HKY-3 shale pressure transmission device, the pressure transmission behavior of different solutions in contact with the Yanchang shale was investigated. The confining pressure was set at 2.3 MPa, the upstream pressure at 1.5 MPa, and the downstream pressure at zero.

2.2.3 Contact angle test

The wettability of shale reservoirs is a crucial petrophysical property that influences fluid distribution, pore migration, and recovery rates. When a liquid droplet contacts a solid surface, the balance of cohesive and adhesive forces shapes the droplet and determines the contact angle (Abdullah et al., 2022), which indicates the rock surface's hydrophilic or hydrophobic nature.

Begin by preparing a standard $20 \times 10 \times 3$ mm thin section. Sand it to create a smooth, scratch-free surface, then rinse with distilled water and dry in an 80 °C oven for 12 h until the weight stabilizes. Immerse the dried shale sections in various solutions for 18 h, then carefully remove them with tweezers and dry in a 50 °C oven for 10 min to remove surface liquid films while minimizing thermal effects on wettability. Next, place a drop of deionized water on the sample surface using a syringe. Measure the contact angle at room temperature with a C2000DM optical contact angle meter. Take measurements at three or more different spots on each sample and calculate the average contact angle.

2.2.4 Surface morphology

To evaluate polymer adsorption and surface coverage on shale, the experiment followed the SY/T 5162-2014, "Methods for Scanning Electron Microscopy Analysis of Rock Samples". Cores samples were ultrasonically cleaned in deionized water, followed by ethanol, for 20 min to remove surface impurities. The samples were then dried at 80 °C until a constant weight was reached.

The cleaned samples were then immersed in a solution containing either 0.4 wt% of hydrophobic associative polymer (SG) or partially hydrolyzed polyacrylamide (PAM) for 18 h. After treatment, the samoles were gently rinsed three times with deionized water and dried at 50 °C for 24 h to prevent thermal degradation while ensuring complete dryness.

The surface morphology of the polymer-treated shale samples was characterized using scanning electron microscopy (SEM) at 2000 times magnification. Multiple representative areas were

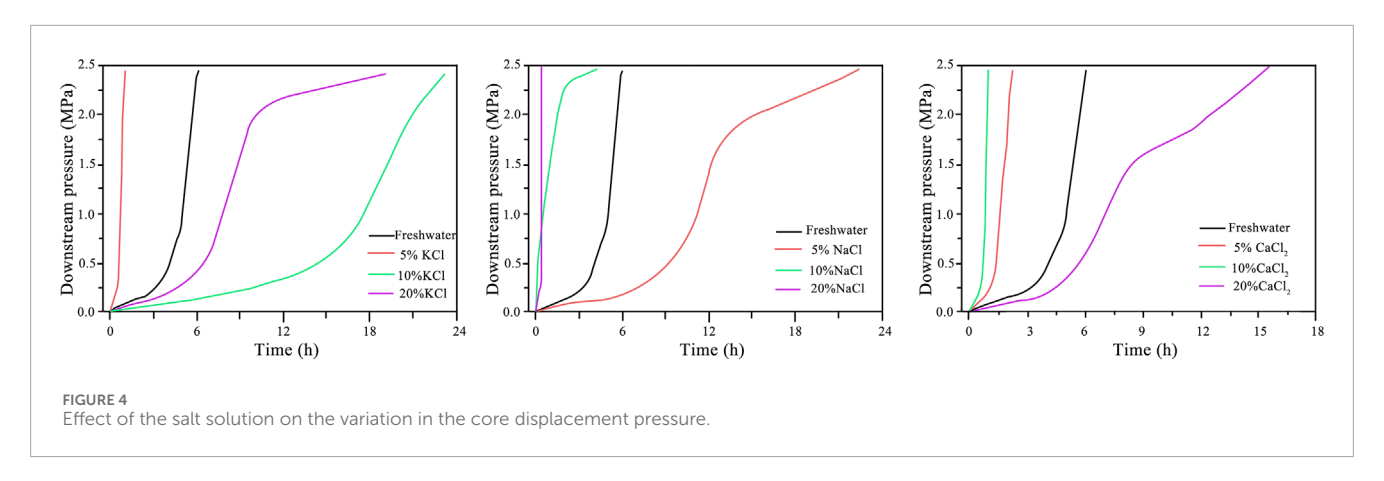


TABLE 1 Changes in shale permeability after different salt invasions.

Solution type	Permeability (×0.01mD)	Permeability damage rate (%)		
5 wt%KCl	45.8	-767.4%		
10 wt%KCl	0.975	81.5%		
20 wt%KCl	1.49	71.8%		
5 wt%NaCl	2.23	57.8%		
10 wt%NaCl	13.3	-151.9%		
20 wt%NaCl	109.1	-1966.3%		
5 wt%CaCl ₂	9.96	-88.6%		
10 wt% CaCl ₂	26.1	-394.3%		
20 wt% CaCl ₂	2.12	59.8%		

examined to ensure comprehensive coverage and statistical reliability.

3 Results and discussion

3.1 Analysis of potential damage mechanisms and measures

3.1.1 Water sensitivity

The average linear swelling of the samples was 14.4 mm, indicating that the shale cores have strong hydration swelling characteristics (Figure 3). The samples swelled rapidly upon initial contact with water, with the swelling rate slowing after 30 min until stabilizing within 6 h. This behavior is mainly due to the high clay mineral content in the shale, which causes moderate water sensitivity.

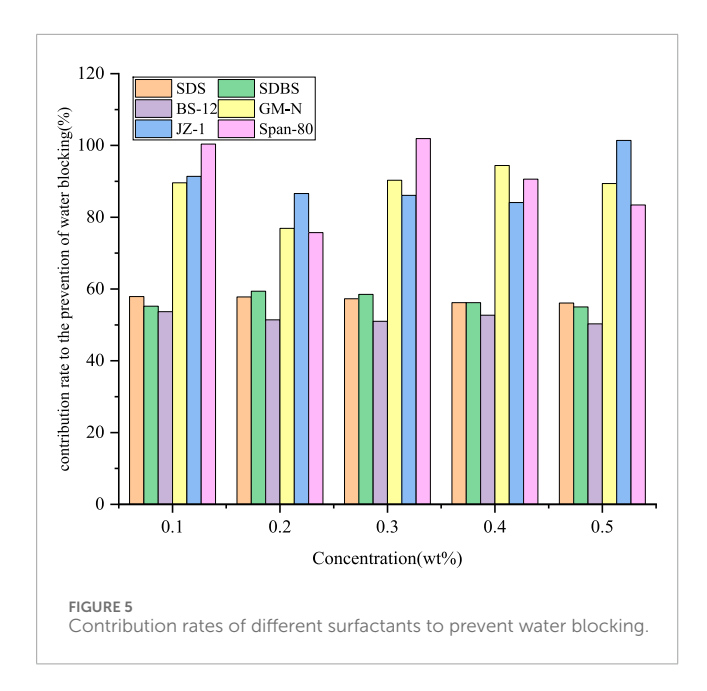
3.1.2 Salt sensitivity

Severe shale spalling occurred repeatedly during drilling of the Chang 7 member of Yanchang. In this study, shale samples were immersed in different concentrations of salt solutions to observe changes in core permeability and assess salt sensitivity. The test fluids

contained 5 wt%, 10 wt%, and 20 wt% of KCl, NaCl and CaCl₂, respectively, with results shown in Figure 4.

As shown in Figure 4, the cores experienced significant permeability damage before immersion in the salt solution, which is attributed to water sensitivity. The effects of chloride solutions on shale core permeability varied widely. Among the potassium chloride solutions tested, the 5 wt% concentration exhibited the highest penetration rate into the shale cores, while the 10 wt% solution showed the slowest rate. The 20 wt% solution demonstrated an intermediate penetration behavior. The migration time increased with concentration but was not directly proportional, mainly due to interactions among water activity, osmotic pressure and clay minerals. This suggests that chloride intrusion causes changes in the original pore structure of the samples. The same irregularity was observed in NaCl and CaCl₂.

In addition, the Chang 7 member of the Yangchang shale contains various brittle minerals, such as clay and quartz, making it susceptible to salt-sensitive damage and resulting irregularities. In this work, permeability recovery tests were conducted on cores after saltwater exposure to evaluate changes in overall pore volume compared to freshwater circulation, and the results are presented in Table 1.



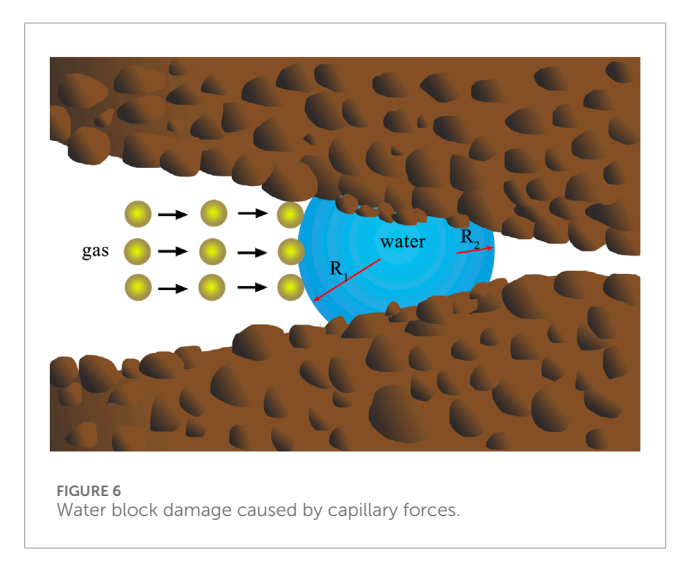


Table 1 highlights the complex effects of salt types and concentrations on shale permeability, which may either enhance or impair flow capacity. Permeability reduction was observed in shale treated with 10 wt% KCl, 20 wt% CaCl₂, and 5 wt% NaCl. Specifically, 10 wt% KCl resulted in an 81.5% decrease in permeability. Although potassium ions are known to inhibit clay swelling, the presence of water-sensitive minerals such as illite and montmorillonite suggests that this concentration may be insufficient to fully suppress hydration. A 20 wt% CaCl₂ solution led to a 59.8% permeability reduction, likely due to excessive salt crystal precipitation under reservoir temperature and pressure, which obstructs pore throats. Similarly, 5 wt% NaCl caused a 57.8% decrease, attributable to the limited inhibition efficiency of sodium ions at low concentration, thereby permitting clay hydration and expansion.

In contrast, negative damage rates indicate permeability enhancement. 10 wt% NaCl resulted in a permeability damage rate of -151.9%, and 20 wt% NaCl further increased permeability

with a damage rate of -1966.3%. This suggests that higher salt concentrations significantly improve flow capacity, a trend also observed in CaCl₂ solutions at specific concentrations.

A comprehensive analysis of both salt type and concentration reveals that different salts may exhibit completely opposite effects under different concentration. As NaCl concentration increases, its impact on shale permeability shifts from impairment to improvement, and eventually to significant enhancement. CaCl_2 exhibits a distinct threshold near 10%, beyond which permeability sharply decreases due to salt precipitation. KCl reverses from significant enhancement to damage as concentration increases, likely due to specific mineral interactions that warrant further investigation.

According to capillary force theory, the water blocking effect in shale reservoirs is governed by the combined influence of fluid surface tension (σ) and rock surface wettability (characterized by the contact angle, θ) (Wang et al., 2022). The contribution rate to the prevention of water blocking effect, denoted as Ψ and defined in Equation 1, provides a quantitative measure of the effectiveness of different surfactants in reducing capillary resistance. In this expression, σ_0 and θ_0 represent the surface tension of pure water and its contact angle on shale surfaces, respectively. Based on experimental measurements of surface tension and contact angles for various surfactants at different concentrations, the contribution rates were calculated and are presented in Figure 5.

$$\Psi = 1 - \frac{\sigma \cos \theta}{\sigma_0 \cos \theta_0} \tag{1}$$

Analysis indicates that all tested surfactants enhance water-blocking performance with contribution rates exceeding 50%, demonstrating their effectiveness in mitigating capillary resistance and reducing water block damage. Cationic surfactants (e.g., GM-N and JZ-1) exhibit particularly high performance, with contribution rates generally above 80% and exceeding 90% at certain concentrations. Their efficacy remains stable across a range of dosages, suggesting consistent performance independent of concentration.

Although anionic surfactants (such as SDS and SDBS) increase shale surface hydrophilicity—resulting in smaller contact angles—they also significantly reduce fluid surface tension, thereby still contributing positively to the prevention of water blocking. The amphoteric surfactant BS-12 shows a relatively low contribution rate, generally between 50% and 54%, with no clear concentration-dependent trend, suggesting its effectiveness is influenced by other factors. Nonionic Span-80 shows a strong capacity to reduce capillary forces, with contribution rates exceeding 100% at certain dosages, but its performance fluctuates considerably, indicating sensitivity to dosage changes.

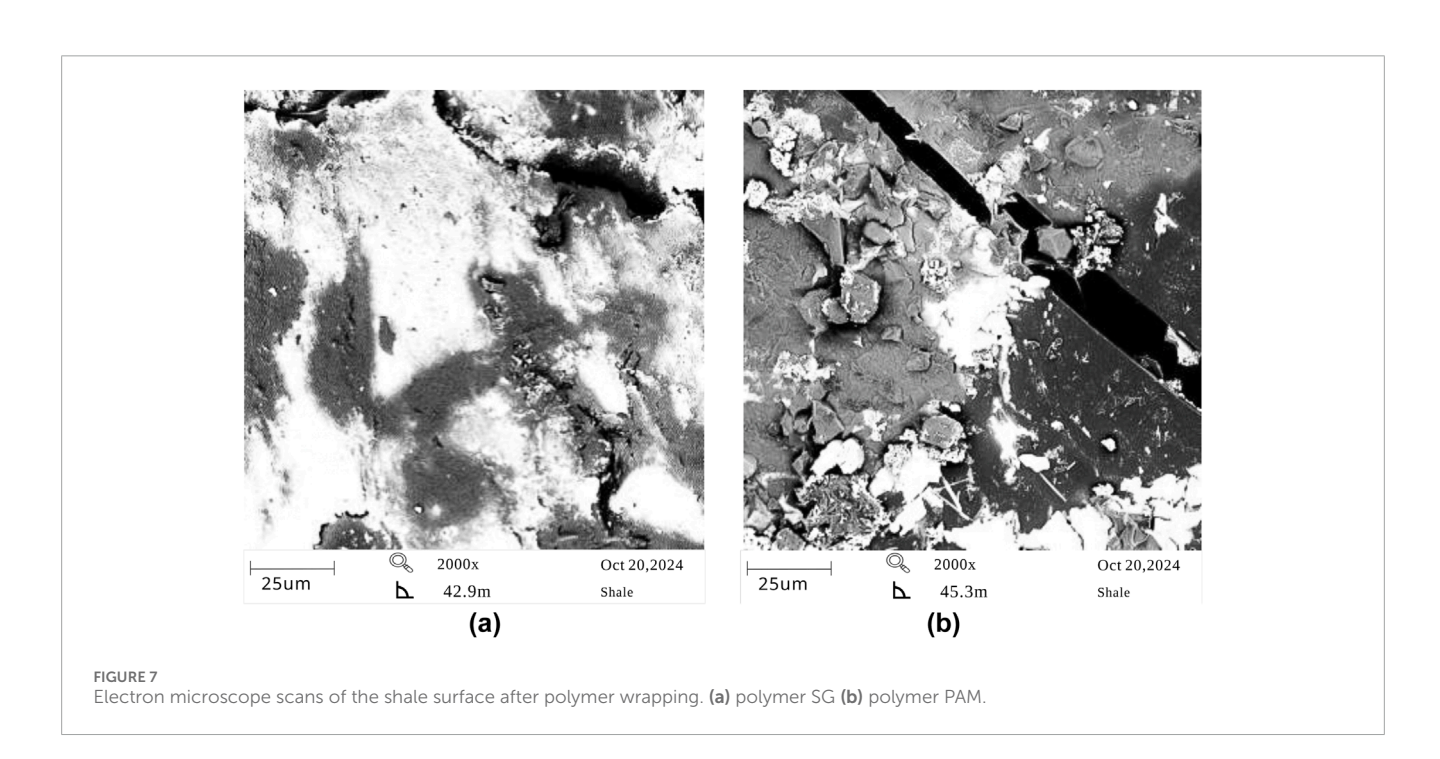
The analysis reveals distinct mechanisms by which surfactant types reduce capillary forces: cationic surfactants maintain high contact angles while effectively controlling surface tension, offering the best overall performance. Anionic surfactants mainly offset the negative effects of altered wettability by significantly lowering surface tension. These findings offer essential guidance for selecting and optimizing water-blocking agents in shale reservoirs.

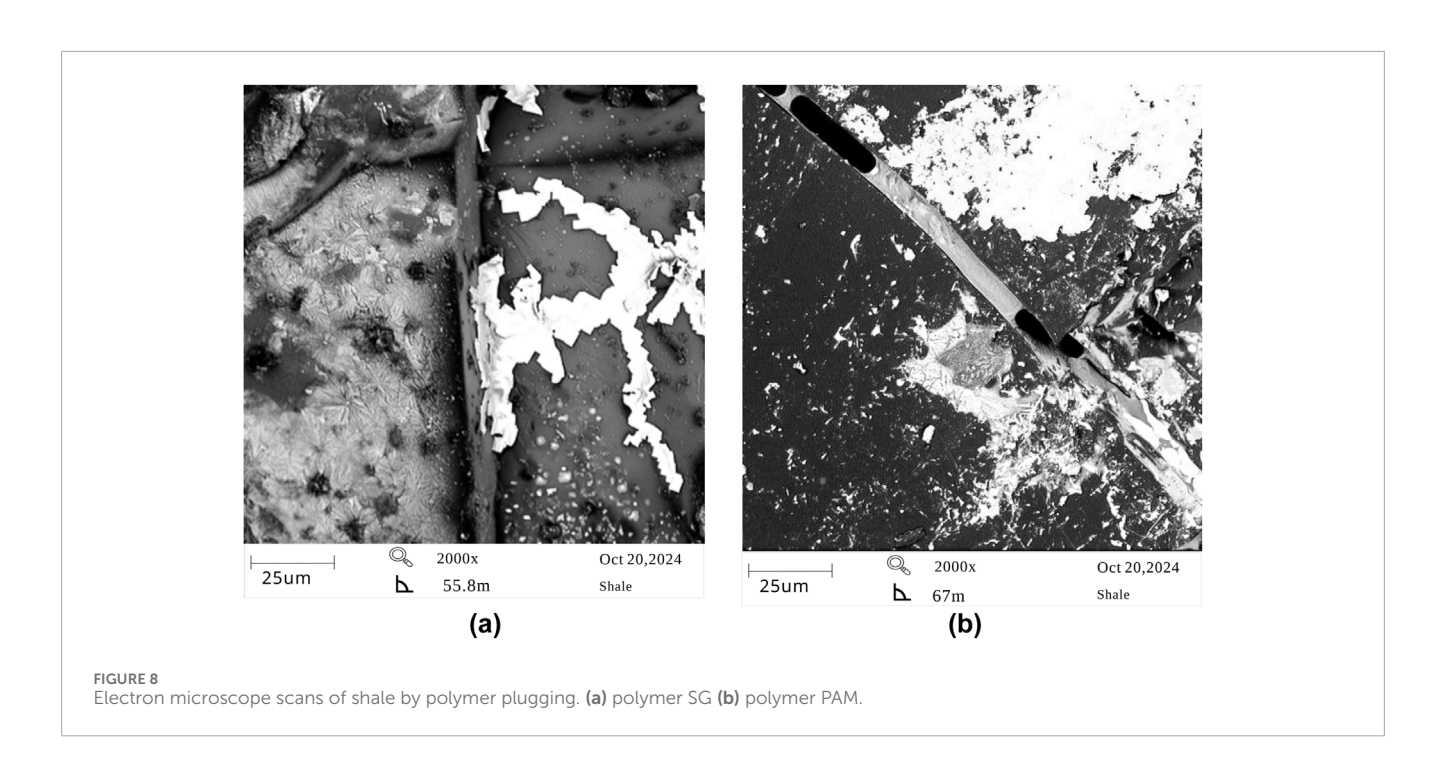
3.1.3 Water blocking

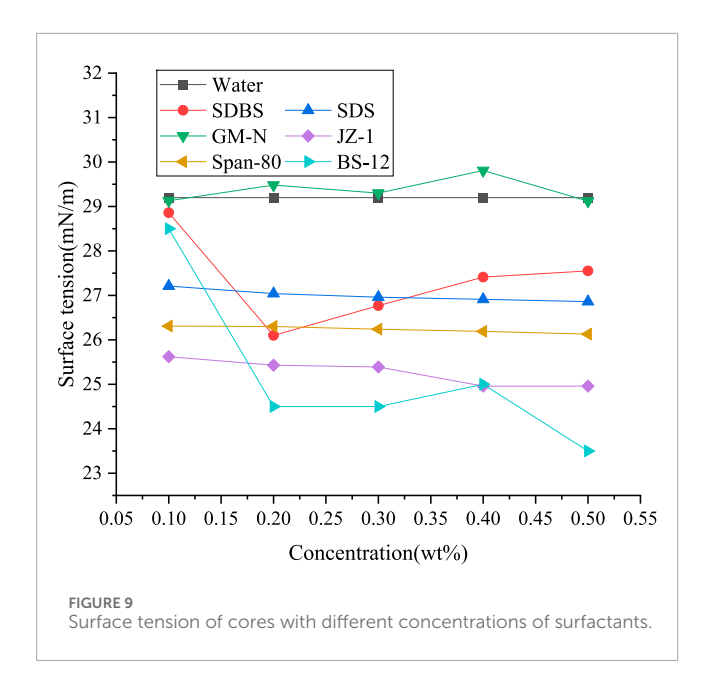
The water blocking effect, a major cause for formation damage in low-permeability shale gas reservoirs, occurs when formation

TABLE 2 Shale permeability before and after freshwater and saltwater circulation.

Fluids	Gas-phase permeability				
	Preexperimental K _{ao} , (nD)	Postexperimental K _{a1} , (nD)	% of decrease		
Case 1: Brine	85.0	23.6	70.4		
Case 2: Fresh water	85	1.7	92.1		







pressure cannot expel foreign fluids, leading to reduced gas permeability (Figure 6). Many studies have shown that large volumes of injected drilling or fracturing fluids can penetrate the formation and cause water-blocking due to high capillary pressures and water-sensitive clays (Sun and Turgay, 2022; Wilson et al., 2014; Van Oort, 1994).

To illustrate the damage caused by water intrusion in shale reservoirs, the shale permeabilities before and after freshwater and saltwater circulation were compared. Table 2 shows that the gas phase permeability of the shale immersed in brine decreased by 70.4%, whereas exposure to circulating freshwater at the core's end and reduced gas-phase permeability by 92.1%. This indicates that water intrusion is the primary cause of damage to the Chang 7 member of the Yangchang shale reservoir.

3.1.4 Polymer invasion

Polymers are commonly used as the main component of water-based drilling and fracturing fluids in shale gas reservoirs to improve fluid rheology and reduce reservoir sensitivity. They adsorb onto shale fracture surfaces at multiple points, preventing gas escape from the matrix surface and lowering the diffusion coefficient. In addition, the diffusion and crossover of polymer molecular chains into reservoir channels hinder gas flow and decrease the gas desorption rate.

The morphological characteristics of polymer adsorption on shale were examined using SEM. Representative images of shale samples treated with polymer solutions is shown in Figure 7.

The white color indicates the polymer encapsulation area, while the black color represents the original sample surface. In Figure 7a, the large white coverage is interconnected, dividing the bare matrix into several separate sections. The polymer SG covers 50% of the whole surface, significantly reducing the effective area for gas desorption. In contrast, the polymer coverage in Figure 7b is more dispersed, and the multipoint adsorption effect of the polymer PAM

is more pronounced than that of SG, with total coverage only about 15% of the surface.

Figure 8 shows the polymer residues in the cracks after immersing the shale cores. Polymer SG not only coated the matrix surface but also filled the fractures, accumulating heavily at the crack top and nearly blocking then entirely. In Figure 8b, polymer PAM penetrated the crack interior and was distributed intermittently along its length. A distinct wetting angle at the crack top indicates that polymer intrusion was driven by capillary forces, significantly reducing the effective volume of the free gas flow channel (Wang et al., 2021; Zhong et al., 2015).

3.2 Optimization of the operating fluid with low damage

Based on the evaluation of potential damage and sensitivity, the damage mechanisms affecting cores in the Yanchang shale include severe water blocking, polymer wrapping and plugging, moderate water sensitivity and salt sensitivity. Drawing from previous studies, the following optimization measures for reservoir damage are proposed.

- 1. To reduce water-blocking damage, surfactants can be added to water-based fracturing fluids to lower the capillary forces in fractures and change the hydrophobicity of shale surfaces.
- Inorganic salts or organic cations enhance fluid inhibition by compressing the diffusion double layer of clay particles. Therefore, ionic treatment agents can provide inhibition while mitigating water-blocking damage.
- For severe polymer invasion, acidification is not recommended due to the environmental concerns. Instead, enzymatic degradation technology can effectively address polymer plugging.

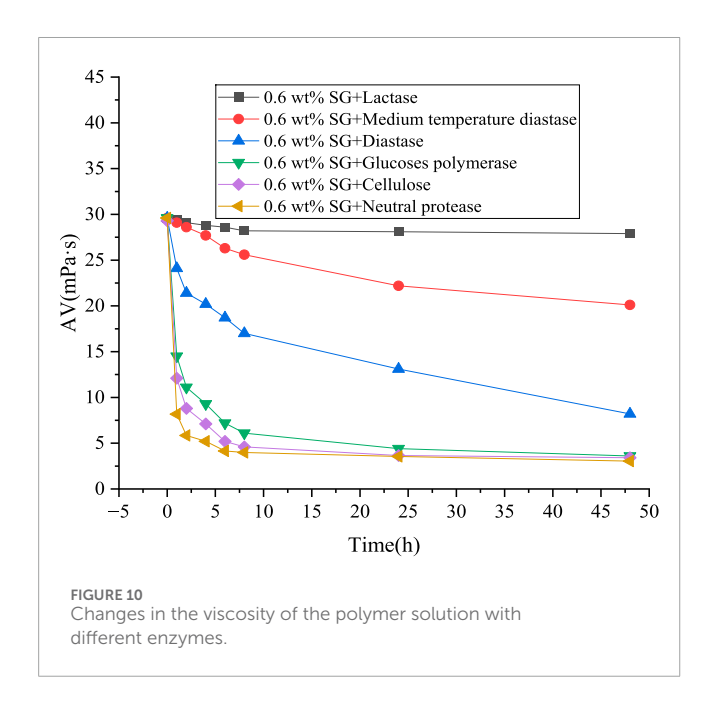
3.2.1 Surfactant optimization

To modify the wettability of shale surfaces, six water-soluble surfactants, were selected for this study: anionic (sodium lauryl sulfate (SDS), sodium dodecyl benzene sulfonate (SDBS)), cationic (quaternary ammonium salts (GM-N, JZ-1)), amphoteric (dodecyl dimethyl betaine (BS-12)) and nonionic (Span80). These surfactants are used as water-locking agents in shale gas reservoir fluids due to their ability to transform the hydrophobic shale surface into a strongly hydrophilic one (Figure 9).

To reduce reservoir damage induced by water blocking during fracturing, enhancing the hydrophobicity of fracturing fluids is critical. Table 3 presents the contact angles of various surfactant-treated fracturing fluids on shale surfaces. As the concentration of anionic surfactants SDBS and SDS increased from 0.1 wt% to 0.5 wt%, the contact angles decreased from 20.5 ° to 9 ° and from 21 ° to 9 °, respectively, indicating enhanced hydrophilicity that hinders water block issues. In contrast, cationic surfactants GM-N and JZ-1 maintained high contact angles at various concentrations (e.g., GM-N reached 83.5 ° at 0.4 wt%, and JZ-1 reached 92 ° at 0.5 wt%), demonstrating

TABLE 3	Contact angle of fractu	urina fluids wit	h various surfactants	on shale surfaces.

Surfactants	0.1 wt%	0.2 wt%	0.3 wt%	0.4 wt%	0.5 wt%	
Fracturing fluid	∠69.2 °					
SDBS	∠20.5 °	∠20°	∠20.5 °	∠15°	∠9°	
SDS	∠21 °	∠19.5 °	∠17°	∠10.5 °	∠9°	
GM-N	∠77.6°	∠61.8 °	∠78.5°	∠83.5 °	∠77.3 °	
JZ-1	∠78.3 °	∠71.5°	∠70.7°	∠67.3 °	∠92°	
Span80	∠90.5	∠56	∠92.5	∠77.5	∠67.5	
BS-12	∠31.83	∠32.26	∠32.51	∠32.69	∠32.71	



strong hydrophobicity characteristics and effective wettability alteration.

This contrast can be attributed to the cationic surfactants' positively charged functional groups, which adsorb onto the negatively charged surfaces of clay minerals through electrostatic interactions. This process forms a stable hydrophobic layer that inhibits water intrusion and reduces the potential for water block damage. The nonionic surfactant Span 80 also showed promising wettability modification, with high contact angles of 90.5° and 92.5° at concentrations of 0.1 wt% and 0.3 wt%, indicating excellent instantaneous hydrophobicity. However, its poor solubility and inconsistent performance at higher concentrations restricts its application. Therefore, in practical fracturing fluid systems, combining Span 80 with ionic surfactants is recommended to enhance hydrophobic stability and solubility, and achieve more effective wetting control and water lock prevention.

3.2.2 Polymer degradant optimization

To obtain polymer degradants for effective degradation, six enzymes were added to the prepared polymer solution (0.6 wt% SG) at a concentration of 0.2 wt‰ and thoroughly mixed. The viscosity changes were measured after 1, 2, 4, 6, 8, 24 and 48 h of standing, as presented in Figure 10.

As shown in Figure 11, cellulose, neutral protease, and glucose polymerase significantly degraded the SG polymer solution. The polymer viscosity decreased by up to approximately 80% within 6 h of enzyme solution.

Metallographic microscopy was employed to observe the polymer residue on the shale surface before and after adding 0.02 wt% cellulose. As shown in Figure 10, most of the polymer covering the shale surface was completely degraded, with only a small amount of residue remaining after 10 min of cellulose treatment.

4 Conclusion

The Chang 7 member of the Yanchang shale is a representative continental shale gas reservoir characterized by low permeability and a dense matrix. Its porosity provides space for shale gas and pathways for intrusive fluids, which can cause formation damage. This study investigated the effects of various salt solutions and polymer fluids, at different concentrations, on the swelling height, permeability, and wettability of the Yanchang shale. Experiments were conducted using a ZNP-1 expansion instrument, an HKY-3 shale pressure transmission device, and a JC2000DM contact angle meter. Based on the results, the following conclusions were drawn.

The shale swelled rapidly upon initial contact with water, then
the swelling height rate gradually slowed, stabilizing after about
6 hours. This moderate water sensitivity is caused mainly by
the high clay mineral content in the Yanchang shale. The
effect of chloride solutions on the shale core permeability
varied significantly. 5 wt% KCl solution penetrated the
core fastest, while 10 wt% KCl solution penetrated slowest,

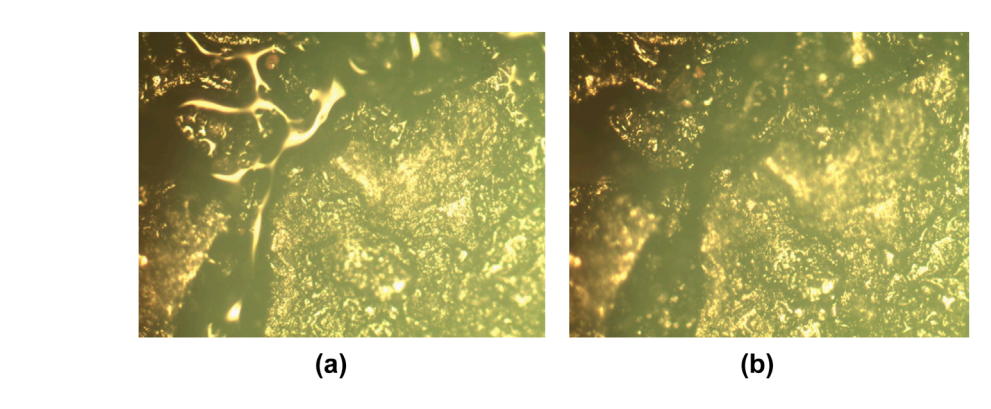


FIGURE 11
Comparison of polymer SGs before and after degradation by cellulose. (a) before degradation (b) after 10 min of degradation.

indicating that chloride intrusion alters the original pore structure.

- Water blocking is the primary and most severe cause of reservoir damage in the Yanchang shale. Introducing surfactants with favorable surface wettability, such as cationic surfactants GM-N and JZ-1, can effectively moderately mitigate water clogging.
- The natural polymer SG significantly blocked the pore structure, preventing free shale gas from flowing out of the reservoir. Using cellulose as a degradation agent effectively reduces the intrusion of polymer SGs.

Data availability statement

The raw data supporting the conclusions of this article will be made available by the authors, without undue reservation.

Author contributions

PL: Conceptualization, Data curation, Formal Analysis, Funding acquisition, Investigation, Methodology, Project administration, Resources, Software, Supervision, Validation, Visualization, Writing – original draft, Writing – review and editing.

Funding

The author(s) declare that financial support was received for the research and/or publication of this article. This work was supported

by Henan Provincial Science and Technology Research Project (252102321104).

Conflict of interest

The author declares that the research was conducted in the absence of any commercial or financial relationships that could be construed as a potential conflict of interest.

Generative AI statement

The author(s) declare that no Generative AI was used in the creation of this manuscript.

Any alternative text (alt text) provided alongside figures in this article has been generated by Frontiers with the support of artificial intelligence and reasonable efforts have been made to ensure accuracy, including review by the authors wherever possible. If you identify any issues, please contact us.

Publisher's note

All claims expressed in this article are solely those of the authors and do not necessarily represent those of their affiliated organizations, or those of the publisher, the editors and the reviewers. Any product that may be evaluated in this article, or claim that may be made by its manufacturer, is not guaranteed or endorsed by the publisher.

References

- Abdullah, A. H., Ridha, S., Mohshim, D. F., Yusuf, M., Kamyab, H., Krishna, S., et al. (2022). A comprehensive review of nanoparticles: effect on water-based drilling fluids and wellbore stability. *Chemosphere* 308, 136274. doi:10.1016/j.chemosphere.2022.136274
- Azim, R. A., Alatefi, S., and Alijehani, A. (2024). A fully coupled thermo-poroelastic model for energy extraction in naturally fractured geothermal reservoirs: sensitivity analysis and flow simulation. *Geotherm. Energy* 12, 26. doi:10.1186/s40517-024-00305-6
- Bal, A., and Misra, S. (2024). Laboratory observation of fluid flow in depleted shale gas reservoir: coupling effect of sorbing and non-sorbing gas on stress, slippage, flow regime in anisotropic and fractured shales. *Energy Fuels*, 38,6868–6890. doi:10.1021/acs.energyfuels.3c05192
- Cadwallader, S., Wampler, J., Sun, T., Sebastian, H., Graff, M., Gil, I., et al. (2015). An integrated dataset centered around a distributed fiber optic monitoring key for the successful implementation of a geoengineered completion optimization program in the eagle ford shale. In: Proceedings of the 3rd unconventional resources technology conference; 2015 July 20-22: San Antonio, Texas, USA. p. 521–531. doi:10.15530/urtec-2015-2171506
- Chaturvedi, K. R., Singh, A. K., and Sharma, T. (2019). Impact of shale on properties and oil recovery potential of sandstone formation for low-salinity waterflooding applications. *Asia-Pacific J. Chem. Eng.* 14 (5), e2352. doi:10.1002/apj.2352
- Chen, M. J., Kang, Y. L., Zhang, X. Y., Lai, Z. H., Li, P. S., and Chen, Z. X. (2021). Evaluation of aqueous phase trapping in shale gas reservoirs based on analytic hierarchy process. *Energy Fuels* 35, 1389–1397. doi:10.1021/acs.energyfuels.0c03867
- Dai, C., Liu, H., Wang, Y. Y., Li, X., and Wang, W. H. (2019). A simulation approach for shale gas development in China with embedded discrete fracture modeling. *Mar. Petroleum Geol.* 100, 519–529. doi:10.1016/j.marpetgeo.2018.09.028
- Duan, M. K., Jiang, C. B., Hu, X. L., Tang, J. Z., Gao, X., Li, W. P., et al. (2022). Study on damage law of raw coal based on different characterization methods. *Adv. Civ. Eng.* 2022, 3129138–11. doi:10.1155/2022/3129138
- Guo, T. K., Gong, F. C., Lin, X., Lin, Q., and Wang, X. Z. (2018). Experimental investigation on damage mechanism of guar gum fracturing fluid to low-permeability reservoir based on nuclear magnetic resonance. *J. Energy Resour. Technol.* 140, 072906–072911. doi:10.1115/1.4039324
- Guo, Z. L., Li, F. F., Liu, Y., and Xiang, J. J. (2022). Development and evaluation of high temperature and low damage fracture fluid. In: *Proceedings of the international field exploration and development conference*. Singapore: Springer. p. 6059–6066. doi:10.1007/978-981-99-1964-2_520
- International Energy Agency IEA (2011). World energy outlook 2011 special report: are we entering a golden age of gas? France: International Energy Agency. Available online at: https://trid.trb.org/view/1119773.
- Li, C., Wang, H., Wang, L., Kang, Y., Hu, K., and Zhu, Y. (2020). Characteristics of tight oil sandstone reservoirs: a case study from the upper Triassic chang 7 member in zhenyuan area, ordos basin, China. *Arabian J. Geosciences* 13, 78. doi:10.1007/s12517-019-4964-1
- Li, P., Hao, Y., Wu, Y., Wanniarachchi, A., Zhang, H. X., and Cai, Z. L. (2023). Experimental study on the effect of $\rm CO_2$ storage on the reservoir permeabilityin a $\rm CO_2$ -based enhanced geothermal system. *Geotherm. Energy* 11, 24. doi:10.1186/s40517-023-00266-2
- Li, Q. (2025). Reservoir science: a multi-coupling communication platform to promote energy transformation, climate change and environmental protection. Reservoir Science 1, 1–2. doi:10.62762/RS.2025.352950
- Li, X. L., Ren, Z. Y., Cao, Z. Z., and Ren, H. (2025a). Study on coal drawing parameters of deeply buried hard coal seams based on PFC. Sci. Rep. 15, 21934. doi:10.1038/s41598-025-08154-4
- Li, Q., Li, Q. C., Wang, F. L., Ning, X., Wang, Y. L., and Bai, B. J. (2025b). Settling behavior and mechanism analysis of kaolinite as a fracture proppant of hydrocarbon reservoirs in $\rm CO_2$ fracturing fluid. *Colloids Surf. A Physicochem. Eng. Asp.* 724, 137463. doi:10.1016/j.colsurfa.2025.137463
- Liu, H., Zhao, Y., Luo, Y., Xiao, G., Meng, Y., Zhou, S., et al. (2020). Origin of the reservoir quality difference between chang 8 and chang 9 member sandstones in the honghe oil field of the southern ordos basin, China. *J. Petroleum Sci. Eng.* 185, 106668. doi:10.1016/j.petrol.2019.106668
- Ngata, M. R., Yang, B. L., Aminu, M. D., Iddphonce, R., Omari, A., Shaame, M., et al. (2022). Review of developments in nanotechnology application for formation damage control. *Energy Fuels* 36, 80–97. doi:10.1021/acs.energyfuels.1c03223

- Nwabia, F. N., and Leung, J. Y. (2024). A practical probabilistic history matching framework for characterizing fracture network parameters of shale gas reservoirs. *Gas Sci. Eng.* 126, 205326. doi:10.1016/j.jgsce.2024.205326
- Shao, L. T., Bai, Y. B., Yang, W. J., Zhang, J. S., Du, C. Z., Zhou, Z. J., et al. (2021). Dynamic characteristics of deposit fracture and impacts of operating pressure during sootblowing in the radiant syngas cooler. *Asia-Pacific J. Chem. Eng.* 16, e2615. doi:10.1002/apj.2615
- Shi, X., Huang, H. Y., Zeng, B., Guo, T. K., and Jiang, S. (2022). Perforation cluster spacing optimization with hydraulic fracturing-reservoir simulation modeling in shale gas reservoir. *Geomechanics Geophys. Geo Energy Geo Resour.* 8, 141. doi:10.1007/s40948-022-00448-5
- Sun, Q., and Turgay, E. (2022). Structure of an artificial-intelligence-assisted reservoir characterization and field development protocol. *Fuel* 324, 124762. doi:10.1016/j.fuel.2022.124762
- Tao, X. J., Gan, M. Z., Yao, Z. H., Bai, J. W., Yang, M. Z., Su, G. D., et al. (2022). Enhancing the production of tight sandstone gas well through fuzzy-ball fluid temporary plugging with diverting fractures and water cutting after refracturing in one operation. *J. Petroleum Sci. Eng.* 217, 110883. doi:10.1016/j.petrol.2022.110883
- Van Oort, E. (1994). A novel technique for the investigation of drilling fluid induced borehole instability in shales. In: *Proceedings of the rock mechanics in petroleum engineering*. Netherlands: Delft. doi:10.2118/28064-MS
- Wang, F. W., Xie, B. Q., Huang, W. A., Cao, J., and Xie, B. Q. (2013). Inhibition comparison between polyether diamine and Quaternary ammonium salt as shale inhibitor in water-based drilling fluid. *Energy Source Part A Recovery Util. Environ. Eff.* 35, 218–225. doi:10.1080/15567036.2011.606871
- Wang, R., Wu, X. M., Li, W. F., Bai, H. T., and Qiao, L. S. (2020). A laboratory approach to predict the water-based drill-in fluid damage on a shale formation. *Energy Explor. Exploitation* 38, 2579–2600. doi:10.1177/0144598720937516
- Wang, L., Zhang, J. G., Jiang, Z. X., Han, C., Luo, D. T., and Zhang, Y. D. (2021). The influence of diagenetic heterogeneity on tight-reservoir properties in the upper Triassic yanchang formation, southeastern ordos basin, China. *Energy Sources* 1-17, 4419–4435. doi:10.1080/15567036.2020.1868624
- Wang, Z., Cao, G. S., Bai, Y. J., Wang, P. L., Wang, X., Liu, X. C., et al. (2022). Construction of sulfur-free gel breaker agent system and investigation on gelbreaking mechanism for association fracturing fluid. *Energy Sources* 44, 5665–5681. doi:10.1080/15567036.2022.2083272
- Wang, L. C., Zhu, L., Cao, Z. Z., Liu, J., Xue, Y., Wang, P. S., et al. (2025). Thermo-mechanical degradation and fracture evolution in low-permeability coal subjected to cyclic heating-cryogenic cooling. *Phys. Fluids* 37, 086617. doi:10.1063/5.0282266
- Wilson, M. J., Wilson, L., and Patey, I. (2014). The influence of individual clay minerals on formation damage of reservoir sandstones: a critical review with some new insights. *Clay Miner.* 49, 147–164. doi:10.1180/claymin.2014. 049.2.02
- Xu, H. L., Jiang, H. S., Wang, J., Wang, T., and Zhang, L. J. (2023). Simulation of fracture propagation law in fractured shale gas reservoirs under temporary plugging and diversion fracturing. *Phys. Fluid* 35, 063309. doi:10.1063/5.0151148
- Yang, X. Y., Shang, Z. X., Shi, Y. P., Peng, Y. D., Yue, Y., Chen, S. Y., et al. (2018). Influence of salt solutions on the permeability, membrane efficiency and wettability of the Lower Silurian longmaxi shale in xiushan, southwest China. *Appl. Clay Sci.* 158, 83–93. doi:10.1016/j.clay.2018.02.006
- Yang, Y. S., Zhang, D. M., and Zhang, F. Y. (2020). Impact of loading-unloading on deformation and permeability of sandstone containing methane. *Energy Sources* 1-18, 10782–10799. doi:10.1080/15567036.2020.1786481
- Yi, J., Liu, L. L., Xia, Z. H., Wang, J. J., Jing, Y., and Duan, L. J. (2021). Effects of wettability on relative permeability of rough-walled fracture at pore-scale: a lattice boltzmann analysis. *Appl. Therm. Eng.* 194, 117100. doi:10.1016/j.applthermaleng.2021.117100
- Zhang, Y., Chen, A., Mao, J. C., Qin, S. H., Li, J., Yang, X. J., et al. (2024). Preparation of a functional fracturing fluid with temperature- and salt-resistance, and low damage using a double crosslinking network. *Petroleum Sci.* 20, 3223–3230. doi:10.1016/j.petsci.2023.04.005
- Zhong, H. Y., Qiu, Z. S., Huang, W. A., Cao, J., Wang, F. W., and Xie, B. Q. (2015). Inhibition properties comparison of different polyetheramines in water-based drilling fluid. *J. Nat. Gas Sci. Eng.* 26, 99–107. doi:10.1016/j.jngse.2015.05.029